ELSEVIER

Physics of the Earth and Planetary Interiors 111 (1999) 123–139

PHYSICS OF THE EARTH AND PLANETARY INTERIORS

Magnetic stability under the magnetostrophic approximation

Douglas R. McLean [a,*], David R. Fearn [b], Rainer Hollerbach [b]

[a] *Laboratoire de Géophysique Interne et Tectonophysique, Université Joseph Fourier, 38041 Grenoble, France*
[b] *Department of Mathematics, University of Glasgow, University Gardens, Glasgow G12 8QW, Scotland, UK*

Received 11 December 1997; accepted 31 July 1998

Abstract

We determine the stability of *s*- and *z*-dependent basic fields under the magnetostrophic approximation in a cylindrical geometry. The geostrophic flow V_G is the dominant nonlinearity in the nonlinear regime. This work assesses the impact of the geostrophic flow at critical linear stability $\Lambda = \Lambda_c$ by imposing V_G as a differential rotation. Here, the Elsasser number Λ is the appropriate nondimensional measure of imposed field strength. Fearn et al. [Fearn, D.R., Lamb, C.J., McLean, D.R., Ogden, R.R., 1997. The influence of differential rotation on magnetic instability and nonlinear magnetic instability in the magnetostrophic limit. Geophys. Astrophys. Fluid Dyn. 86, 173–200] showed that for simple *s*-dependent basic fields, certain imposed differential rotations could lower Λ_c. McLean and Fearn [McLean, D.R., Fearn, D.R., 1999. The geostrophic nonlinearity and its effect on magnetic instability. Geophys. Astrophys. Fluid Dyn., In Press.] then showed that the geostrophic flow-induced subcritical behaviour in the most unstable mode for various combinations of basic fields and aspect ratios. Here, both linear and nonlinear results are new; previous analyses only considered radially (*s*-)dependent basic fields. We will derive a consistency condition necessary for the existence of solutions before investigating whether subcriticality exists under a dipolar basic field configuration.

Keywords: Geomagnetic field; Geostrophic flow; Cylindrical geometry

1. Introduction

It is generally accepted that the geomagnetic field is generated from the liquid iron outer core of the Earth. There, field sustaining fluid motions perpetuate the nonlinear geodynamo mechanism. Measurement of the strength of the Earth's magnetic field is made difficult since the toroidal component vanishes at the core–mantle boundary (CMB). It is only the poloidal part which can be measured at the Earth's surface. Thus, the precise strength of the geomagnetic field in the core is not known. However, strong field theory predicts that the toroidal component will be stronger than its poloidal counterpart (see Fearn, 1997).

The recent explosion in computer technology has allowed the formulation and numerical solution of dynamo problems which, until recently, were not numerically tractable. In particular, we are now able to formulate and solve geodynamo models. This task is made especially difficult owing to a result by Cowling (1934). He showed that a purely axisymmetric magnetic field cannot be supported by dynamo action. This has profound implications for any

* Corresponding author. E-mail: douglas.mclean@obs.ujf-grenoble.fr

0031-9201/99/$ - see front matter
PII: S0031-9201(98)00151-4

self-consistent dynamo model in that it must be three-dimensional and memory and speed limitations become very real. However, Glatzmaier and Roberts (1995a,b, 1996, 1997) and Kuang and Bloxham (1997a,b) have successfully integrated their respective dynamo models through a number of diffusion time scales

$$\tau_\eta = \mathscr{L}^2/\eta = O(10^5) \text{ years}. \tag{1.1}$$

Here, η is the magnetic diffusivity and $\mathscr{L}$ is a typical lengthscale (e.g., the outer core radius). It should be stressed, however, that the models cited are greatly limited by the smallness of viscosity in the Earth's outer core. Terrestrial estimates put the Ekman number

$$E = \nu/2\,\Omega_0\,\mathscr{L}^2 = O(10^{-15}). \tag{1.2}$$

The Ekman number E is a nondimensional measure of the viscosity ν and an inverse measure of the Earth's angular frequency Ω_0. In fact, the smallest value that is at present computationally possible puts $E = O(10^{-4})$ which, although small, is much larger than geophysical values. A common feature of self-consistent dynamo models is the use of 'hyperdiffusivities' associated with the viscosity ν and the magnetic diffusivity η. The hyperdiffusivities are designed to damp small-scale structures, which can lead to numerical instability, more heavily than the larger-scale structures. It is a great shame that hyperdiffusivities are necessary, since they obscure the true value of the Ekman number and do not help us to better understand the nonpassive role of the Ekman boundary layers in the evolution of the geodynamo.

Given the problems cited, we realise that if progress is to be made in understanding the geodynamo, it is absolutely necessary that all avenues of research be pursued. In particular, simpler model problems which retain aspects of the physics will complement the full 3D models and lead to a better understanding of the underlying mechanisms at work. In this paper, we do not concern ourselves with the generation of the main (or basic) field, but consider its stability to small perturbations. Any instabilities found are important since they will give constraints on the unknown field and sustain motions in the core.

Much work has been done involving magnetic instabilities. In fact, the subject enjoys an extensive literature (see, e.g., Acheson, 1972, 1973, 1983; Zhang and Fearn, 1994, 1995) and is closely related to magnetoconvection. There, instabilities are driven in the presence of an imposed temperature field. Zhang (1995b) has shown that magnetically driven and thermally driven instabilities are part of the same mechanism. Thus, it makes sense to simplify the problem and focus on instabilities driven solely by the basic magnetic field. Fearn (1983a,b, 1984, 1985, 1988) has completed linear magnetic stability analysis of azimuthal basic state fields of the form

$$\mathbf{B}_0^* = B_\mathrm{M}\mathbf{B}_0 = B_\mathrm{M}\, sF(s)\mathbf{1}_\phi \tag{1.3}$$

in rapidly rotating cylindrical geometries. Here B_M is the maximum field strength of the (imposed) basic state field $\mathbf{B}_0^*$, (s,ϕ,z) are the system of cylindrical polar coordinates and $\mathbf{1}_s$, $\mathbf{1}_\phi$, $\mathbf{1}_z$ are the corresponding base vectors. Starred variables refer to dimensional quantities and unstarred variables, to their dimensionless counterparts [see (2.5) and the associated text for an explanation of the nondimensionalisation]. Under the magnetostrophic approximation, inertial and viscous terms are neglected from the momentum equation (2.2). This is done on the grounds that the leading order force balance is between Lorentz, Coriolis and buoyancy forces. Fearn has shown that instabilities often manifest themselves when the Elsasser number

$$\Lambda \equiv B_\mathrm{M}^2/2\,\Omega_0\,\mu_0\,\rho\eta = O(1). \tag{1.4}$$

Here, μ_0 is the magnetic permeability of free space, ρ is the constant density of the core fluid (it is constant, since we consider an isothermal fluid independent of temperature) and η is the magnetic diffusivity. Such values of the Elsasser number are not inconsistent with geomagnetic observations and with the current theory that the Earth contains a strong, hidden, toroidal field, where $\Lambda = O(1)$ and a weaker poloidal field emerging at the Earth's surface, where $\Lambda < O(1)$. Therefore, magnetic instabilities will play a role in the evolution of the geodynamo.

Typically, in magnetic stability analysis, one begins by decomposing the magnetic and flow fields

into their respective axisymmetric $(\overline{\mathbf{B}}^*, \overline{\mathbf{V}}^*)$ and non-axisymmetric parts $(\mathbf{b}^*, \mathbf{v}^*)$:

$$\mathbf{B}^*(s,\phi,z,t) = \overline{\mathbf{B}}^*(s,z,t) + \mathbf{b}^*(s,\phi,z,t)$$

$$\mathbf{V}^*(s,\phi,z,t) = \overline{\mathbf{V}}^*(s,z,t) + \mathbf{v}^*(s,\phi,z,t). \quad (1.5)$$

For a vector function $\mathbf{F}$, we define its axisymmetric $\overline{\mathbf{F}}$ and non-axisymmetric $\mathbf{f}$ parts by

$$\overline{\mathbf{F}} = \frac{1}{2\pi}\int_0^{2\pi} \mathbf{F}\,\mathrm{d}\phi \text{ and } \mathbf{f} = \mathbf{F} - \overline{\mathbf{F}}. \quad (1.6)$$

Once the substitutions (1.5) have been made, then the governing equations decouple into separate evolution equations for the axisymmetric and non-axisymmetric components (see Fearn, 1994). To compute a linear stability analysis, one may then prescribe the (mean) axisymmetric field as a basic state $(\overline{\mathbf{B}}^* = \mathbf{B}_0^*, \overline{\mathbf{V}}^* = \mathbf{V}_0^*)$ and solve only the non-axisymmetric equations for the instabilities $(\mathbf{b}^*, \mathbf{v}^*)$. When we move beyond the linear regime, nonlinear feedback on the mean field from the instability exists. However, after an order analysis, it may be possible to neglect part of this feedback depending on the precise amplitudes of $(\mathbf{b}^*, \mathbf{v}^*)$. In particular, if the amplitudes of the instabilities approach amplitudes in the Ekman regime $[O(E^{1/4})]$, then as we will show in Section 3.2, a mean poloidal field $\mathbf{B}_\mathrm{P}^* = O(E^{1/2})$ is generated. Since $|\mathbf{B}_\mathrm{P}^*| \ll |\mathbf{b}^*|$, then it may be neglected explicitly from the non-axisymmetric equations under an order analysis. However, $\mathbf{B}_\mathrm{P}^*$ does make a first-order contribution to the geostrophic flow $V_\mathrm{G}\mathbf{1}_\phi$ (see below) and, hence, its contribution to V_G cannot be ignored. This is an important point to make, since the geostrophic flow is the dominant nonlinear effect in the Ekman regime and controls the class of bifurcation into the nonlinear state. [As the amplitude of instability moves beyond $O(E^{1/4})$ and approaches $O(1)$, we move into the Taylor regime and any solution there must satisfy Taylor's condition

$$\int_{C(s^*)} \left[(\nabla^* \times \mathbf{B}^*) \times \mathbf{B}^*\right]_\phi \mathrm{d}S^* \quad (1.7)$$

at leading order. Here, $C(s^*)$ is any concentric cylinder centred on the axis of rotation. For a full description of Taylor States and Ekman States see, e.g., Taylor (1963), Malkus and Proctor (1975), Jault (1995) or Hollerbach (1996).]

In earlier work, Fearn et al. (1997), McLean (1997) and McLean and Fearn (1999) (hereafter referred to as FLMO, M97 and MF98, respectively) investigated the nonlinear development of linear instabilities of the basic state (1.3) found by Fearn (1988). M97 and MF98 utilised the magnetostrophic approximation in the fluid main body, but reintroduced viscosity into the Ekman boundary layers next to the flat top and bottom bounding plates in their annular model. The instabilities were then considered at finite amplitudes $O(E^{1/4})$ in the Ekman regime. Since V_G is the dominant nonlinearity in the Ekman state, they simplified their problem significantly by neglecting all other nonlinearities. This has meant that any solutions found must be of the Ekman type. M97 and MF98 have also shown that when the cylindrical annular geometry is used, the two flat plate no-normal-flow boundary conditions become degenerate. Then, the traditional form for the geostrophic flow

$$V_\mathrm{G}(s,t)\mathbf{1}_\phi = \frac{(2E)^{-1/2}}{2\pi s^*}\int_{C(s^*)} \left[(\nabla^* \times \mathbf{B}^*) \times \mathbf{B}^*\right]_\phi \times \mathrm{d}S^*\,\mathbf{1}_\phi, \quad (1.8)$$

converted from its form in the sphere for the cylindrical geometry, only forms part of the flow. In fact, in the cylindrical geometry, there exists a non-axisymmetric component of the geostrophic flow. They assert that the geostrophic flow must be of the form

$$V_\mathrm{G}^s(s,\phi,t)\mathbf{1}_s + \left[V_\mathrm{G}^\phi(s,\phi,t) + \overline{V_\mathrm{G}^\phi}(s,t)\right]\mathbf{1}_\phi. \quad (1.9)$$

The form (1.9) necessarily implies that the numerical problem be fully three-dimensional when we consider basic states of the form

$$\mathbf{B}_0^* = B_\mathrm{M} sF(s)G(z)\mathbf{1}_\phi \quad (1.10)$$

rather than being two-dimensional in a similar problem within a spherical geometry. We therefore neglect the non-axisymmetric component of the geostrophic flow

$$V_\mathrm{G}^s(s,\phi,t)\mathbf{1}_s + V_\mathrm{G}^\phi(s,\phi,t)\mathbf{1}_\phi \quad (1.11)$$

for numerical tractability and for geophysical realism (the non-axisymmetric component of the geostrophic flow cannot exist in the geophysically relevant spher-

ical geometry). Hutcheson and Fearn (1995a,b) (hereafter HF1,2) considered problems similar with those of M97 and MF98, but with the addition of viscosity throughout their annular geometry. Following on from their work, Hutcheson and Fearn (1996, 1997) (hereafter HF3,4) considered the linear and nonlinear stability of basic states of the form (1.10). In our magnetostrophic problem, neglecting (1.11) has the implication that we must be very cautious when comparing our results with the corresponding results of HF3,4. The presence of viscosity in their problem has meant that the geostrophic flow is calculated implicitly within the flow field. As we will see in Section 4, the cylindrical geometry (or, indeed, any Cartesian geometry) under the magnetostrophic approximation leads to a consistency condition for the existence of solutions.

This paper is organised as follows: in Section 2, we discuss the magnetohydrodynamic stability problem which we solve, first, by detailing the geometry and evolution equations. Then, a consistency condition for the existence of solutions will be derived in Section 4 before moving onto the results in Section 5. There, we consider the linear stability and primary bifurcation class of dipole basic states of the form (1.10). Finally, we discuss the implications of our results in Section 6.

2. Magnetohydrodynamic problem

2.1. Bounded annular model

Using cylindrical polar coordinates (s^*,ϕ,z^*), our model consists of a cylindrical annulus $\mathscr{A}^*$ of inner and outer radii s_i and s_o, respectively, bounded in axial extent by flat, horizontal plates $z^* = \pm d$. The annular region

$$\mathscr{A}^* = \{(s^*,\phi,z^*): s_i < s^* < s_o, |z^*| < d\} \qquad (2.1)$$

is filled with an incompressible, isothermal conducting fluid of constant density ρ_0 and rapidly rotates with angular frequency Ω_0 about the z^*-axis. This work represents the natural continuation from the previous work done by MF98. There, we were able to compare the stability results of basic states of the form (1.3) with the corresponding viscous analyses of Hutcheson and Fearn (1995a,b). In this paper, we compare the stability results of dipole fields which take the form (1.10) with the viscous analysis of Hutcheson and Fearn (1996, 1997).

2.2. Governing equations

The time-evolution of an isothermal, electrically conducting fluid with velocity $\mathbf{V}^*$ and its associated magnetic field $\mathbf{B}^*$ is governed by the momentum and magnetic induction equations. These, together with the fluid incompressibility constraint and the divergence free condition for the magnetic field complete our hydromagnetic system (although the divergence free condition is not independent from the magnetic induction equation). In dimensional form, these are:

$$\rho_0\left[\frac{\partial \mathbf{V}^*}{\partial t} + \mathbf{V}^*\cdot\nabla^*\mathbf{V}^*\right] + 2\Omega_0 1_z \times \mathbf{V}^* = -\nabla^* \Pi^* + \nu\nabla^{*2}\mathbf{V}^* + \mu^{-1}(\nabla^*\times\mathbf{B}^*)\times\mathbf{B}^*, \qquad (2.2)$$

$$\frac{\partial \mathbf{B}^*}{\partial t} = \nabla^*\times(\mathbf{V}^*\times\mathbf{B}^*) + \eta\nabla^{*2}\mathbf{B}^*. \qquad (2.3)$$

$$\nabla^*\cdot\mathbf{V}^* = \nabla^*\cdot\mathbf{B}^* = 0. \qquad (2.4)$$

We nondimensionalise length on the outer annular radius s_o. The conducting fluid is then confined to the annular region $\mathscr{A} = \{(s,\phi,z): s_{ib} < s < 1, |z| < \zeta\}$, where $s_{ib} = s_i/s_o$ and $\zeta = d/s_o$. In this work, we take $s_{ib} = 0.35$ and $\zeta = \pi/2$. Time is scaled with the slow magnetohydrodynamic (or dynamo) time scale

$$\tau_s = 2\Omega_0/\Omega_M^2, \qquad \Omega_M^2 = B_M^2/s_o^2\mu\rho. \qquad (2.5)$$

Here, Ω_M is the Alfvén frequency. The magnetic field is scaled by its maximum amplitude B_M as $\mathbf{B}^* = B_M\mathbf{B}$ and the flow as $\mathbf{V}^* = s_o\mathbf{V}/\tau_s$. We then decompose the magnetic and flow field as

$$\mathbf{B}(s,\phi,z,t) = \mathbf{B}_0(s,z) + \nabla\times\left[A(s,z)\mathbf{1}_\phi\right] + \mathbf{b}(s,\phi,z,t)$$
$$\mathbf{V}(s,\phi,z,t) = \mathbf{V}_0(s,z) + \mathbf{V}_M(s,z) + V_G(s)\mathbf{1}_\phi + \mathbf{v}(s,\phi,z,t), \qquad (2.6)$$

where $(\mathbf{B}_0,\mathbf{V}_0)$ is the basic state field and flow, A is the induced mean poloidal field [it is neglected ex-

plicitly from the perturbation equations (2.8), (2.9) and (2.10), but makes a first-order contribution to the geostrophic flow; see Section 3.2] and (**b**,**v**) is the (non-axisymmetric) instability. The basic state magnetic field $\mathbf{B}_0$ induces the magnetic wind

$$\mathbf{V}_M = \int_{z'=z}^{z_T} \nabla \times \left[(\nabla \times \mathbf{B}_0) \times \mathbf{B}_0 \right] dz' = O(1) \quad \left[z_T = (1-s^2)^{1/2} \right]$$

(see, e.g., Fearn, 1997). However, it was found in the subsequent calculations that the results with $\mathbf{V}_M$ were not significantly different from the results without $\mathbf{V}_M$. We therefore omit further discussion of the magnetic wind and write

$$\mathbf{V}(s,\phi,z,t) = V_G(s)\mathbf{1}_\phi + \mathbf{v}(s,\phi,z,t), \tag{2.7}$$

since we have not prescribed any basic state flow ($\mathbf{V}_0 = \mathbf{0}$). Substituting the perturbation forms (2.6) and (2.7) into the nondimensionalised governing equations and neglecting all nonlinear terms except where V_G is involved, yields the perturbation equations

$$\Lambda \mathrm{Ro}\left[\frac{\partial \mathbf{v}}{\partial t} + \left(V_G \mathbf{1}_\phi\right) \cdot \nabla \mathbf{v} + \mathbf{v} \cdot \nabla\left(V_G \mathbf{1}_\phi\right) \right] + \mathbf{1}_z \times \mathbf{v} = -\nabla \pi + E\nabla^2 \mathbf{v} + (\nabla \times \mathbf{B}_0) \times \mathbf{b} + (\nabla \times \mathbf{b}) \times \mathbf{B}_0, \tag{2.8}$$

$$\frac{\partial \mathbf{b}}{\partial t} = \nabla \times (\mathbf{v} \times \mathbf{B}_0) + \nabla \times \left(V_G \mathbf{1}_\phi \times \mathbf{b}\right) + \Lambda^{-1}\nabla^2 \mathbf{b}, \tag{2.9}$$

$$\nabla \cdot \mathbf{b} = \nabla \cdot \mathbf{v} = 0, \tag{2.10}$$

where $\mathrm{Ro} = \eta/2\Omega_0 d^2$ is the Rossby number. Given the fact that $|\mathrm{Ro}|, |E| \ll O(1)$, we make an approximation which is nearly magnetostrophic: $\mathrm{Ro} = 0$ and $0 < E \ll 1$. This means that fluid inertia may be neglected from (2.8) and an order analysis allows us to neglect the viscous force. However, viscosity will be significant in the boundary layers and this is accommodated through the modified Taylor's condition. Thus, any solution found will implicitly incorporate the viscous effects from the boundary layers and be valid everywhere in the inviscid interior of $\mathscr{A}$.

2.3. Boundary conditions and solution expansions

Under the magnetostrophic approximation, the governing equations drop from being tenth order in s to fourth order. This complicates the choice of boundary conditions along the curved annular sidewalls. First, all normal components of the flow must vanish along the surfaces $s = s_{ib}, 1$. Second, for the magnetic field, perfect electrical insulators inhabit the regions exterior to the annulus: $s < s_{ib}$ and $s > 1$. Third, along the insulating sidewalls, there must be no normal current and the field interior to the annulus must match to an external potential field. This requires six conditions to be satisfied on $s = s_{ib}, 1$ when the differential order in s is only 4. Fortunately, Fearn (1983a) has shown that the two no-normal-flow conditions on the sidewalls can be met with the addition of a viscous layer. This leaves us free to enforce no-normal-current flow and to match the interior field to an external potential field at $s = s_{ib}, 1$.

On $z = \pm\zeta$, the boundary conditions are the no normal flow and perfect electrical conductor conditions:

$$\mathbf{n} \cdot \mathbf{v} = 0, \ \mathbf{n} \cdot \mathbf{b} = 0 \text{ and } \mathbf{n} \times \mathbf{e} = 0 \text{ on } z = \pm\zeta. \tag{2.11}$$

Written here in its dimensional form, Ohm's law allows us to eliminate the perturbed electric field $\mathbf{e}^*$:

$$\mathbf{e}^* = \sigma^{-1}\mathbf{j}^* - \mathbf{v}^* \times \mathbf{B}_0^* = \eta\nabla^* \times \mathbf{b}^* - \mathbf{v}^* \times \mathbf{B}_0^*,$$

where σ is the electrical conductivity and $\mathbf{j}^*$ is the perturbed current density. From the boundary condition on the electric field, we then have the two conditions

$$\frac{\partial b_z}{\partial s} = \frac{\partial b_s}{\partial z} \text{ and } \frac{1}{s}\frac{\partial b_z}{\partial \phi} = \frac{\partial b_\phi}{\partial z} + u_z B_0.$$

However, at either top or bottom boundary, the normal component of flow must vanish. Therefore,

$$\frac{\partial b_z}{\partial \phi} = s\frac{\partial b_\phi}{\partial z}.$$

For the boundary conditions on the perfectly conducting plates at $z = \pm\zeta$, a Galerkin technique is employed.

$$X(s,\phi,z,t) = \sum_{n=0}^{NZ} X_n(s,t)\cos\bar{n}(z+\zeta)e^{im\phi} + \text{CC}, \tag{2.12}$$

$$Y(s,\phi,z,t) = \sum_{n=0}^{NZ} Y_n(s,t)\sin\bar{n}(z+\zeta)e^{im\phi} + \text{CC}, \tag{2.13}$$

where X represents any of v_s, v_ϕ, b_s or b_ϕ and Y represents either v_z or b_z. The variable $\bar{n} = n\pi/2\zeta$, where $0 \le n \le NZ$. In here, we have used a truncation of $NZ = 8$.

Considering the regions exterior to the annular volume, these regions $0 \le s \le s_{ib}$ and $s \ge s_{ib}$ are solid insulators and there can be no current flow present. Therefore, from Maxwell's equations, we find $\nabla \times \mathbf{b} = 0$ in $s < s_{ib}$ and $s > 1$. Consequently, the exterior magnetic field $\mathbf{b}^e$ may be described by a magnetostatic scalar potential field $U = U(s,\phi,z)$

$$\mathbf{b}^e = -\nabla U. \tag{2.14}$$

Using the divergence free condition, U must satisfy Laplace's equation $\nabla^2 U = 0$. Therefore, the magnetic field interior to the annulus must match to an external potential field. Following a similar procedure as in Fearn (1988), one can show that the magnetic match conditions reduce to

$$sDb_{s,0} + (1-m)b_{s,0} = 0 \quad \text{on } s = s_{ib}, \tag{2.15}$$

$$sDb_{s,0} + (1+m)b_{s,0} = 0 \quad \text{on } s = 1. \tag{2.16}$$

for the zeroth mode $n = 0$. For $n > 0$, the match conditions are simply

$$b_{s,n}(s,t) = \gamma_n b_{z,n}(s,t) \qquad \text{for } 1 \le n \le NZ, \tag{2.17}$$

where

$$\gamma_n = \begin{cases} -\left[\dfrac{I_{m+1}(\bar{n}s_{ib})}{I_m(\bar{n}s_{ib})} + \dfrac{m}{\bar{n}s_{ib}}\right] & \text{if } s = s_{ib} \\ \left[\dfrac{K_{m+1}(\bar{n})}{K_m(\bar{n})} - \dfrac{m}{\bar{n}}\right] & \text{if } s = 1, \end{cases} \tag{2.18}$$

where $\bar{n} = n\pi/2\zeta$. Here, I_m and K_m are modified Bessel functions (see Chap. 9 of Abramowitz and Stegun, 1965).

For the condition that there be no normal current flow across either boundary, $j_s = (\nabla \times \mathbf{b})_s = 0$ requires that

$$\frac{1}{s}\frac{\partial b_z}{\partial \phi} - \frac{\partial b_\phi}{\partial z} = 0 \qquad \text{on } s = s_{ib}, 1. \tag{2.19}$$

Using $\nabla \cdot \mathbf{b} = 0$ to obtain an expression for b_ϕ in terms of b_s and b_z, we substitute this back into (2.19) and obtain

$$s^2 Db_{s,n} + sb_{s,n} + [\bar{n}^2 s^2 + m^2]b_{z,n}/\bar{n} = 0 \quad \text{on } s = s_{ib}, 1 \text{ for } 1 \le n \le NZ. \tag{2.20}$$

3. The basic state, the mean poloidal field and the geostrophic flow

3.1. The basic state

We study the stability of basic s- and z-dependent axisymmetric field configurations of the form (1.10) to non-axisymmetric perturbations (**b**,**v**) within the geometry of a bounded annular container (2.1). Inclusion of a z-dependence in the basic field configuration is geophysically realistic, but leads to a more complicated problem formulation, since the axial modes may no longer be considered in isolation as in MF98. In this work, the presence of the independent variable z in the perturbation equations (2.8), (2.9) and (2.10) couples the axial modes together and the problem becomes fully two-dimensional. As a result, extensive modifications have been made to the computer program used for MF98, so that it may accommodate a wider range of basic toroidal fields.

Zhang and Fearn (1994) assessed the linear stability of toroidal field configurations in the spherical shell geometry. There, problems of resolution were encountered and the annular geometry is the logical alternative that is more tractable. As already mentioned in the introduction, our magnetostrophic study complements the work of HF1–4 who solved the same stability problem, but at finite Ekman number. They did not use the magnetostrophic approximation and included many other nonlinear interactions neglected in our analysis. HF1,2 considered the stability of radially dependent basic state fields which are best compared with results in MF98, whereas HF3,4 examined s- and z-dependent basic (azimuthal) fields (1.10) which we consider in this paper.

In each stability analysis conducted in the past, either by Fearn (1983b, 1984, 1985, 1988), HF1–4,

or FLMO, the s-dependence has always been taken in the form (3.1). For this, the field is concentrated towards the CMB. However, field concentration towards the ICB may be equally important. To this end, we also consider the stability of s- and z-dependent basic fields whose radial dependence is given in (3.2). The choices (3.1) and (3.2) allow us to compare the stability results arising from different field profiles: one concentrating towards the CMB and one towards the ICB. Contour plots showing meridional sections of the (axisymmetric) basic fields are shown in Fig. 1. The radial dependencies, $F(s)$, are given as

$$F(s) = \left[2/\left(1 - s_{\mathrm{ib}}^4\right)\right]^2 (1 - s^4)\left(s^4 - s_{\mathrm{ib}}^4\right) \tag{3.1}$$

$$F(s) = \left[2/\left(1 - s_{\mathrm{ib}}^4\right)\right]^2 \left(1 - (1 + s_{\mathrm{ib}} - s)^4\right) \times \left((1 + s_{\mathrm{ib}} - s)^4 - s_{\mathrm{ib}}^4\right). \tag{3.2}$$

The function $G(z)$ contains the z-dependence of the basic field. Therefore, the z-independent fields of MF98 correspond to taking $G = 1$. In this paper, G is chosen to have an equatorially antisymmetric field symmetry about the equator $z = 0$. Here, we use the nomenclature of Gubbins and Zhang (1993) (equatorially symmetric E^{S} or equatorially antisymmetric E^{A} parities) to identify symmetries about the equator. We consider the following functional dependence

$$G(z) = \cos \bar{l}(z + \zeta), \qquad \text{where } \bar{l} = l\pi/2\zeta. \tag{3.3}$$

By taking l odd (even) leads to an equatorially antisymmetric E^{A} (symmetric E^{S}) basic field. In this work, we report the simplest dipolar case

$$\mathrm{E}^{\mathrm{A}}: l = 1. \tag{3.4}$$

It should be noted that although we use a pure dipole basic field here, our problem has been formulated, so that any basic field may be considered.

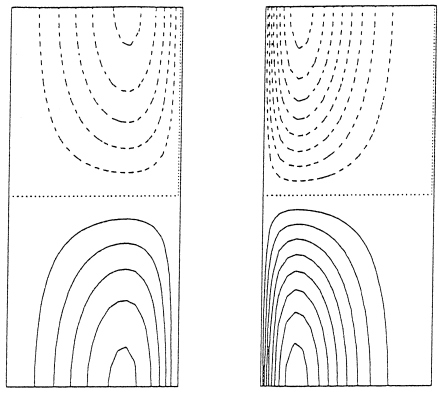

Fig. 1. Meridional sections of the basic dipolar field $\mathbf{B}_0$ using G defined by (3.3) and (3.4). Left to right: (i) using F from (3.1), (ii) using F from (3.2).

3.2. The contribution to V_G from the mean poloidal field

When the instabilities (**b**,**v**) reach amplitudes of $O(E^{1/4})$ (i.e., in the Ekman regime), a mean poloidal field $\mathbf{B}_{\mathrm{P}} = O(E^{1/2})$ will be generated through the action of the electromotive force [this can be seen from the source term on the right-hand side of (3.6)]. The mean part of the magnetic field is then

$$\overline{\mathbf{B}} = \mathbf{B}_0(s,z) + \mathbf{B}_{\mathrm{P}} = B_0(s,z)\mathbf{1}_\phi + \nabla \times \left(A\mathbf{1}_\phi\right), \tag{3.5}$$

where we have written the induced poloidal field $\mathbf{B}_{\mathrm{P}}$ in terms of its poloidal scalar A. The evolution of A is described by

$$\frac{\partial A}{\partial t} + \left(\frac{1}{s^2} - \nabla^2\right) A = \overline{\left[\mathbf{v} \times \mathbf{b}\right]}_\phi \tag{3.6}$$

(see Fearn, 1994). Since the amplitudes of the instabilities are $O(E^{1/4})$ then $A = O(E^{1/2})$ and, consequently, may be neglected in the linear problem. Whilst A is $O(E^{1/4})$ smaller than the magnitude of **b**, the induced poloidal field cannot, in general, be neglected in calculating the geostrophic flow.

Observe that

$$V_{\mathrm{G}} = (2E)^{-1/2} \int_{-\zeta}^{\zeta} \overline{\left[(\nabla \times \mathbf{B}) \times \mathbf{B}\right]}_\phi \, \mathrm{d}z \equiv V_{\mathrm{G}}^{(\mathrm{pol})} + V_{\mathrm{G}}^{(\mathrm{inst})}, \tag{3.7}$$

where the contribution from the mean poloidal field is

$$V_{\mathrm{G}}^{(\mathrm{pol})} = (2E)^{-1/2} \int_{-\zeta}^{\zeta} \left[(\nabla \times \overline{\mathbf{B}}) \times \overline{\mathbf{B}}\right]_\phi \mathrm{d}z \tag{3.8}$$

and the corresponding contribution from the magnetic instabilities is

$$V_G^{(inst)} = (2E)^{-1/2} \int_{-\zeta}^{\zeta} \overline{[(\nabla \times \mathbf{b}) \times \mathbf{b}]}_{\phi} \mathrm{d}z. \quad (3.9)$$

By seeking instabilities (**b**,**v**) in the Ekman regime, then $V_G^{(inst)}$ contributes at first order to the geostrophic flow. As is shown in M97:

$$V_G^{(inst)} = \left(\frac{2}{E}\right)^{\frac{1}{2}} \sum_{n=0}^{NZ} \alpha_n \Re\left(s^{-1} b_{s,n} + b_{s,n} D - \bar{n} b_{z,n}\right) \times b'_{\phi,n}, \quad (3.10)$$

where the prime denotes the complex conjugate and

$$\alpha_n = \begin{cases} 2\zeta & \text{if } n = 0 \\ \zeta & \text{if } n > 0. \end{cases} \quad (3.11)$$

The integrand contained in (3.8) may be written as

$$\left[(\nabla \times \bar{\mathbf{B}}) \times \bar{\mathbf{B}}\right]_{\phi} = -\frac{\partial A}{\partial z} \frac{1}{s} \frac{\partial}{\partial s}(sB_0) + \frac{\partial B_0}{\partial z} \frac{1}{s} \frac{\partial}{\partial s}(sA). \quad (3.12)$$

Since $A = O(E^{1/2})$, then the mean field must also, in general, make an $O(1)$ contribution to V_G. If the basic field is z-independent ($G = 1$), as taken by FLMO, then

$$\int_{-\zeta}^{\zeta} \left[\frac{\partial A}{\partial z} \frac{1}{s} \frac{\partial}{\partial s}(sB_0) - \frac{\partial B_0}{\partial z} \frac{1}{s} \frac{\partial}{\partial s}(sA)\right] \mathrm{d}z = \left[\frac{A}{s} \frac{\partial}{\partial s}(sB_0)\right]_{-\zeta}^{\zeta} = 0.$$

This result is independent of the form for F. However, if B_0 is also z-dependent, then the integral of (3.12) is not necessarily zero.

$$(2E)^{1/2} V_G^{(pol)} = \int_{-\zeta}^{\zeta} \left[(\nabla \times \bar{\mathbf{B}}) \times \bar{\mathbf{B}}\right]_{\phi} \mathrm{d}z = -\left[\frac{A}{s} \frac{\partial}{\partial s}(s^2 FG)\right]_{-\zeta}^{\zeta} + \int_{-\zeta}^{\zeta} \frac{A}{s} \frac{\mathrm{d}}{\mathrm{d}s}(s^2 F) G' + FG' \frac{\mathrm{d}}{\mathrm{d}s}(sA) \mathrm{d}z. \quad (3.13)$$

By writing

$$A = \sum_{k=1}^{\infty} A_k(s) \sin \bar{k}(z + \zeta), \quad (3.14)$$

the boundary conditions on $z = \pm\zeta$ for the poloidal field, i.e., $\mathbf{1}_z \cdot \mathbf{B}_P = 0$ on $z = \pm\zeta$, are satisfied. Continuing from (3.13) and substituting the form (3.3) for $G(z)$:

$$\begin{aligned} &-\bar{l} \sum_{k=1}^{\infty} \int_{-\zeta}^{\zeta} \left[\frac{A_k}{s} \frac{\mathrm{d}}{\mathrm{d}s}(s^2 F) + F \frac{\partial}{\partial s}(sA_k)\right] \\ &\times \sin \bar{k}(z + \zeta) \sin \bar{l}(z + \zeta) \mathrm{d}z \\ &= \frac{\bar{l}}{2} \sum_{k=1}^{\infty} \left[\frac{A_k}{s} \frac{\mathrm{d}}{\mathrm{d}s}(s^2 F) + F \frac{\mathrm{d}}{\mathrm{d}s}(sA_k)\right] \\ &\times \int_{-\zeta}^{\zeta} \left[\cos(\bar{k} + \bar{l})(z + \zeta) \right. \\ &\left. - \cos(\bar{k} - \bar{l})(z + \zeta)\right] \mathrm{d}z. \end{aligned} \quad (3.15)$$

Provided $\bar{k} \neq \bar{l}$, then (3.15) will vanish. Therefore, $\bar{k} = \bar{l}$ makes the only nonzero contribution and we have

$$(2E)^{1/2} V_G^{(pol)} = \frac{l\pi}{2s^2} \frac{\mathrm{d}}{\mathrm{d}s}\left(s^3 F A_l\right) \quad (3.16)$$

where l takes the value 1 according to the basic state selected [see (3.4)].

In order to find the poloidal scalar A, we must solve

$$\left(\frac{\partial}{\partial t} + \frac{1}{s^2} - \frac{\partial^2}{\partial s^2} - \frac{1}{s} \frac{\partial}{\partial s} + \bar{k}^2\right) A_k = \sum_{r,n=0}^{\infty} f_{rn}\{\delta_{k-n,r} + \gamma_{k,n,r}\} \quad (3.17)$$

for all $k \geq 1$, where $\delta_{k-n,r}$ is the Kronecker delta symbol,

$$\gamma_{k,n,r} = \begin{cases} \zeta & \text{if } \bar{r} \neq \bar{n} - \bar{k} \text{ and } \bar{r} = \bar{n} + \bar{k} \\ -\zeta & \text{if } \bar{r} = \bar{n} - \bar{k} \text{ and } \bar{r} \neq \bar{n} + \bar{k} \\ 0 & \text{if } \bar{r} \neq \bar{n} - \bar{k} \text{ and } \bar{r} \neq \bar{n} + \bar{k} \end{cases} \quad (3.18)$$

and, where a prime denotes the complex conjugate,

$$f_{r,n}(s) = \Re(v_{z,r} b'_{s,n} - v_{s,n} b'_{z,r}) \quad (3.19)$$

It should be pointed out that, under the magnetostrophic approximation, the perturbation equations (2.8), (2.9) and (2.10) do not determine the radial flow component corresponding to the zeroth axial mode $v_{s,0}$ [see (2.12)]. The zeroth axial mode is actually the non-axisymmetric part of the radial geostrophic flow [see (1.8)]

$$v_{s,0} = V_G^s - \overline{V_G^s}, \tag{3.20}$$

where $\bar{F} = \int_0^{2\pi} F \mathrm{d}\phi/2\pi$. Further work is needed to resolve V_G^s and hence $v_{s,0}$. At present, however, we set $v_{s,0} \equiv 0$, since our motivation for examining this magnetic stability problem is that much of the physics will carry over to a similar problem in a spherical shell geometry.

3.3. Enforcing V_G as a differential rotation at $\Lambda = \Lambda_c$

When examining the class of primary bifurcation into the nonlinear regime, under z-independent basic states, M97 and MF98 input the geostrophic structure $V_G^{(0)}\mathbf{1}_\phi$, calculated once from (3.10) using the linear eigenfunction found at $\Lambda = \Lambda_c$, as the differential rotation

$$\mathscr{R}_m V_G^{(0)}\mathbf{1}_\phi \tag{3.21}$$

in their time-stepping calculations. For small values of the modified magnetic Reynolds' number, e.g., we have taken $\mathscr{R}_m = V_m\tau_s/s_o \cong O(10^{-3})$ (where V_m is the maximum amplitude of the differential rotation), the behaviour of the differential rotation (3.21) gives, to an excellent approximation, the behaviour of the nonlinear geostrophic flow. (In fact, the smaller $\mathscr{R}_m$ is, the better the approximation.) Thus, the type of primary bifurcation into the nonlinear regime could be determined easily in a linear calculation by examining the change in the growth rate of the magnetic field when (3.21) was incorporated at neutral stability.

In the spirit of enforcing a differential rotation with the geostrophic structure computed from the linear eigenfunction at $\Lambda = \Lambda_c$, we sketch how the contribution from the mean field may also be included in the differential rotation.

The steady state version of Eq. (3.17)

$$\left(\frac{1}{s^2} - \frac{\partial^2}{\partial s^2} - \frac{1}{s}\frac{\partial}{\partial s} + \bar{k}^2\right) A_k = \frac{1}{2}\sum_{r,n=0}^{\infty} f_{rn}\{\delta_{k-n,r} + \gamma_{k,n,r}\} \tag{3.22}$$

was solved with the linear eigenfunctions **b** and **v** substituted into f_{rn}. Since a Galerkin method has enabled us to satisfy the perfectly conducting boundary conditions on the top and bottom flat bounding plates $z = \pm\zeta$, and since $\mathbf{B}_P$ does not induce any normal current $\bar{\mathbf{J}}_s$ at the curved annular surfaces $s = s_{ib}$, 1, we need only ensure that the poloidal field match to an external potential field at $s = s_{ib}$, 1. This is achieved by solving Laplace's equation for the exterior magnetic potential $V_P^{(e)}$ in a similar fashion to that already done earlier for the magnetic instability **b** (see Fearn, 1988). The match conditions are

$$\frac{\mathrm{d}A_k}{\mathrm{d}s} + \left(\frac{1}{s} + \frac{\bar{k}}{\gamma_{P,k}}\right) = 0 \tag{3.23}$$

where

$$\gamma_{P,k} = \begin{cases} -\dfrac{I_1(\bar{k}s_{ib})}{I_0(\bar{k}s_{ib})} & \text{if } s = s_{ib} \\ \dfrac{K_1(\bar{k})}{K_0(\bar{k})} & \text{if } s = 1. \end{cases} \tag{3.24}$$

Finally, we were required only to solve (3.22) for the values $k = 1$ in the case of our dipolar basic state field. Once A_k was obtained, it was substituted into (3.16) to obtain the mean poloidal field contribution to V_G. This was then added to the non-axisymmetric contribution to the geostrophic flow and at that point, the sum was scaled by the magnetic Reynolds' number ready to be input as a differential rotation.

4. Consistency condition

Consider the perturbation form of the magnetostrophic momentum equation

$$\mathbf{1}_z \times \mathbf{v} = -\nabla\pi + (\nabla \times \mathbf{B}_0) \times \mathbf{b} + (\nabla \times \mathbf{b}) \times \mathbf{B}_0. \tag{4.1}$$

If one takes the z-component of the curl of (4.1), then

$$-\frac{\partial v_z}{\partial z} = \left\{\nabla \times \left[(\nabla \times \mathbf{B}_0) \times \mathbf{b} + (\nabla \times \mathbf{b}) \times \mathbf{B}_0\right]\right\}_z. \tag{4.2}$$

Now, the no-normal-flow boundary conditions require that $v_z = 0$ on $z = \pm\zeta$. Therefore,

$$\int_{-\zeta}^{\zeta} \frac{\partial v_z}{\partial z} \mathrm{d}z = \left[v_z\right]_{-\zeta}^{\zeta} = 0.$$

Consequently, any solution we find must satisfy the consistency relationship

$$\int_{-\zeta}^{\zeta} \left\{\nabla \times \left[(\nabla \times \mathbf{B}_0) \times \mathbf{b} + (\nabla \times \mathbf{b}) \times \mathbf{B}_0\right]\right\}_z \mathrm{d}z = 0 \tag{4.3}$$

$$\begin{aligned} \Leftrightarrow \int_{-\zeta}^{\zeta} \Bigg\{ & \frac{1}{s}\frac{\partial}{\partial s}\left[b_s \frac{\partial}{\partial s}(sB_0)\right] + \frac{1}{s}\frac{\partial}{\partial s}\left[sb_z \frac{\partial B_0}{\partial z}\right] \\ & + \frac{1}{s^2}\frac{\partial b_\phi}{\partial \phi}\frac{\partial}{\partial s}(sB_0) + \frac{B_0}{s^2}\frac{\partial^2}{\partial s \partial \phi}(sb_\phi) \\ & - \frac{B_0}{s^2}\frac{\partial^2 b_s}{\partial \phi^2}\Bigg\} \mathrm{d}z = 0. \end{aligned} \tag{4.4}$$

On appealing to (2.12), we see that if the basic field is z-independent, as was taken by FLMO or MF98, $[B_0 = sF(s)]$, then (4.4) will always be satisfied.

However, if we take $B_0 = sF(s)G(z)$ as is done in this work with $G(z)$ selected from (3.4), then it is not clear whether upon making the substitutions (2.12) and (2.13) that (4.4) will be satisfied. This issue can partly be resolved in the following way. Each term in (4.4) will be proportional to either

$$\begin{aligned} G(z)\cos\bar{n}(z+\zeta) &= \frac{1}{2}\left[\cos(\bar{n}+\bar{l})(z+\zeta)\right. \\ &\quad \left. + \cos(\bar{n}-\bar{l})(z+\zeta)\right] \\ G'(z)\sin\bar{n}(z+\zeta) &= -\frac{1}{2}\left[\cos(\bar{n}+\bar{l})(z+\zeta)\right. \\ &\quad \left. - \cos(\bar{n}-\bar{l})(z+\zeta)\right] \end{aligned}$$

where $\bar{n} = n\pi/2\zeta$, $n \in [0,1,2,\ldots)$ and a prime indicates the z-derivative. Consider the dipole field configuration created by choosing $l = 1$ [see (3.4)] for $G(z)$. Provided the most unstable instability is quadrupolar in nature, then it is the even modes n which are selected and, consequently, (4.4) must vanish. A similar result exists if one chooses $l = 2$ (i.e., a quadrupolar basic field) and the dipolar instability. However, it is not clear as to whether (4.4) will or will not be satisfied if either of the other two combinations of basic field and instability are selected. In this event, we cannot say anything about our results and they are not quoted.

This represents a serious deficiency in cylindrical models under the magnetostrophic approximation even in the *linear* regime. In order to address this problem, further work is needed. The restoration of a some form of viscosity to the right-hand side of the magnetostrophic momentum equation (4.1) may help to resolve the problem.

5. Results

The stability problem was solved by an LU-decomposition method applied to a part spectral and part finite-difference discretization of the governing equations. As in MF98, a semi-implicit method was employed incorporating the Crank–Nicholson scheme for the diffusive terms and an Adams–Bashforth method for the remaining terms.

The computations ran on a Silicon Graphics R10000 Workstation. Although run times lasted, at most, half an hour, it usually took several runs to determine a single critical parameter value Λ_c. Such values were found by starting with either arbitrary or 'previous solution' initial conditions and time stepping long enough to establish growth or decay of the solution (see M97 or MF98). Once the appropriate trend had been determined, the parameter values were varied and the process was repeated. After two such computations were completed, a secant method could be applied in the remaining cycles to find the zero Λ_c of the growth rate of the magnetic energy.

We found it useful to redefine the Elsasser number Λ in terms of the mean field energy density rather than by a field's maximum amplitude. M97 and MF98 defined the 'energetic Elsasser number' as

$$\Lambda' = \frac{E^*(\mathbf{B}_0^*)}{2\Omega_0\rho_0\mu\eta} = \frac{B_M^2}{2\Omega_0\rho_0\mu\eta} E(\mathbf{B}_0) = E(\mathbf{B}_0)\Lambda. \tag{5.1}$$

Here, $E^*(\mathbf{B}_0^*)$ is the dimensional mean field energy density which is related to its dimensionless form by

$$E^*(\mathbf{B}_0^*) = \frac{1}{\mathrm{Vol}^*(\mathscr{A}^*)}\int_{\mathscr{A}^*}\mathbf{B}_0^*\cdot\mathbf{B}_0^*\,\mathrm{d}V^* = \frac{B_\mathrm{M}^2}{\mathrm{Vol}(\mathscr{A})}\int_{\mathscr{A}}\mathbf{B}_0\cdot\mathbf{B}_0\mathrm{d}V = B_\mathrm{M}^2 E(\mathbf{B}_0). \tag{5.2}$$

A redefinition of Λ in terms of the basic field energy $E(\mathbf{B}_0)$ facilitates a realistic comparison between the different field configurations that we consider. In this paper, all critical Elsasser numbers are quoted for the energetic version Λ' [but note that Λ values may be retrieved upon using (5.1)].

The results are organised as follows: first, we consider the dipole field concentrating towards the CMB in Section 5.1 before considering the field concentrating towards the ICB in Section 5.2. In each case, the geostrophic structure is applied at neutral stability to determine the sub or supercriticality of the system into the Ekman regime (see Section 3.3). Note, also, that in order to satisfy the consistency condition, see Section 4, we are forced to consider only instabilities of the quadrupolar type (for the dipole basic state). We therefore set to zero the dipolar instabilities and force the quadrupolar parity.

5.1. Dipole field (CMB)

The stability results for the dipole field are detailed in Table 1 below. A field profile for the dipolar axisymmetric basic state can be located in Fig. 1.

The results for the first five azimuthal modes, considered in isolation due to the separability in ϕ, are shown. The higher azimuthal modes are significantly more damped by ohmic diffusion than those shown here and are, consequently, not quoted. Since the z-dependent basic fields have weaker average field strengths than their z-independent counterparts (MF98), use of Λ' allows a realistic comparison between each basic field. The values of Λ'_c corresponding to the z-independent field using (3.1) are the correct comparison with the results in this paper and are shown in italics in Table 1.

Table 1
Critical parameter values for the dipole field with values for the z-independent field shown italicised

m	1	2	3	4	5
Λ'_c	2.381	0.8159	0.5256	0.4955	0.5816
	1.392	*0.6909*	*0.5615*	*0.5864*	–
ω_c	−0.8963	0.6835	−5.227	−11.93	−19.78
Modes	$\mathscr{E}$	$\mathscr{E}$	$\mathscr{E}$	$\mathscr{E}$	$\mathscr{E}$
Bifurcation	Sub	Sub	Sub	Sub	Sub

Here, the only difference between the basic fields is in the form for G: the z-dependent case (3.4) vs. the z-independent case where $G=1$. On inspection of Table 1, we see that the introduction of a z-dependence has had a destabilising effect.

The most unstable mode for the dipolar basic field is the $m=4$, quadrupolar Q-instability with frequency -11.93. Comparison of our most unstable $m=4$ mode contrasts with the similar, but viscous results of HF3 which suggest that $m=2$ is the preferred mode. This prompted us to rework our problem for their aspect ratio of $\zeta=1$, but there was little difference from the results when $\zeta=\pi/2$ (hence, they are not reproduced).

In the manner of MF98, we use the linear eigenfunction at neutral stability ($\Lambda'=\Lambda'_\mathrm{c}$) to generate the geostrophic flow $V_\mathrm{G}^{(0)}(s)$ (see Section 3.2). Normalising that flow and modulating it with the modified magnetic Reynolds' number and enforcing the flow as a differential rotation allows us to determine the initial effect of V_G on the solution in the nonlinear regime. (Typically, we set $\mathscr{R}_\mathrm{m}=10^{-3}$.) In contrast with the results of HF4 who did not find subcritical instability, we find that the geostrophic flow has an inherently destabilising nature with the most unstable modes forming subcritical instabilities [this result was mirrored for quadrupolar basic state where $l=2$ in (3.3)].

The real and imaginary parts of the linear solution **b** and **v** [see (2.12) and (2.13)] are represented in Figs. 2 and 3. Meridional sections, drawn as contour plots, show the structure of the most unstable, $m=4$, mode at $\Lambda'_\mathrm{c}=0.4955$. The eigenfunctions for **b** and **v** have been normalised separately, but in the same way. For example, the field was normalised by dividing by the quantity

$$\sum_{n=0}^{NZ}\left(b_{z,n}^\mathrm{r}+ib_{z,n}^\mathrm{i}\right)\sin\bar{n}(z+\zeta)\exp(im\phi) \tag{5.3}$$

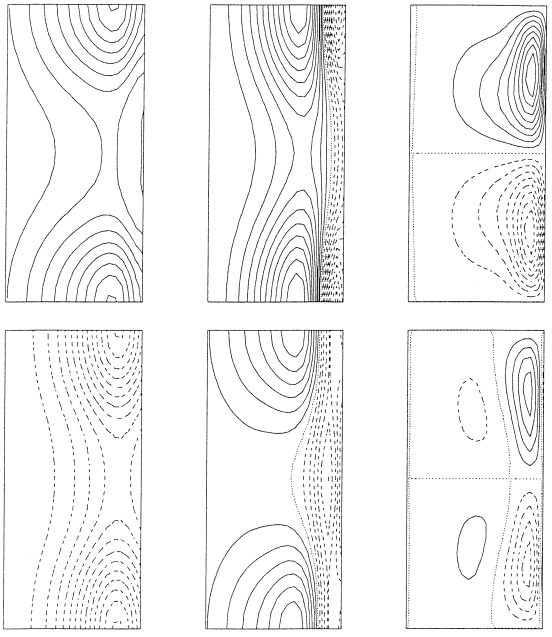

Fig. 2. The perturbed magnetic field **b**. Meridional sections maximising over ϕ for the most unstable $m=4$ mode under the dipole field configuration in Fig. 1(i). Top row, from left to right: the real part of (i) b_s, (ii) b_ϕ and (iii) b_z. The bottom row is as the top row, but shows the corresponding imaginary parts. All figures use the same contour interval.

evaluated at the point $P=(s_{\max},\phi_{\max},z_{\max})$. Here, a superscript r/i refers to the real/imaginary part. P was found as the point which maximised the real part of b_z, i.e., P is the point for which

$$\Re(b_z)=\sum_{n=0}^{NZ}\left(b^{\mathrm{r}}_{z,n}\cos m\phi-b^{\mathrm{i}}_{z,n}\sin m\phi\right)\times\sin\bar{n}(z+\zeta), \tag{5.4}$$

where

$$\phi=m^{-1}\arctan\left(-b^{\mathrm{i}}_{z,n}/b^{\mathrm{r}}_{z,n}\right) \tag{5.5}$$

is a maximum.

The first observation that can be made is that the instability, as one intuitively expects, tends to concentrate in the region close to the CMB (towards the right-hand side of the plots). The quadrupolar nature of the instability is also evident. The plots are well-resolved showing large scale structure occurring on length scales over the radius of the annulus. The corresponding geostrophic flow structure is shown in Fig. 4. There, the two contributions to the geostrophic flow: the mean poloidal field's contribution $V_{\mathrm{G}}^{(\mathrm{pol})}$ and the magnetic instability's contribution $V_{\mathrm{G}}^{(\mathrm{inst})}$; are shown separately and whose sum is V_{G}. Under this section's particular choice of dipolar field concentrating toward the CMB, one can see that it is the contribution from the mean field $V_{\mathrm{G}}^{(\mathrm{pol})}$ which dominates the geostrophic flow. However, for the basic dipole field concentrating toward the ICB, it is the contribution from the magnetic instability $V_{\mathrm{G}}^{(\mathrm{inst})}$ which dominates V_{G} [see (3.7)].

A useful check of our results is to evaluate the expression

$$I=\int_{s_{\mathrm{ib}}}^{1}s^2V_{\mathrm{G}}(s)\,\mathrm{d}s. \tag{5.6}$$

This condition is identical to Eq. 17 of Jault (1995) when his half height z_1 is taken to be a constant (as

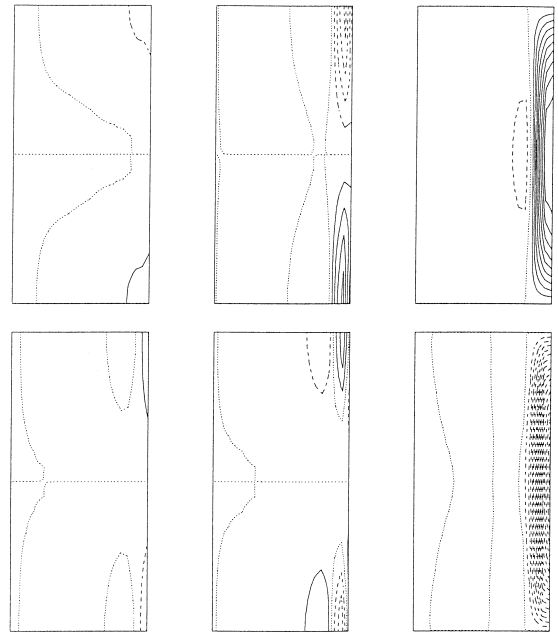

Fig. 3. The perturbed flow field **v**. Meridional sections maximising over ϕ for the most unstable $m=4$ mode under the dipole field configuration in Fig. 1(i). Top row, from left to right: the real part of (i) v_s, (ii) v_ϕ and (iii) v_z. The bottom row is as the top row, but shows the corresponding imaginary parts. All figures use the same contour interval.

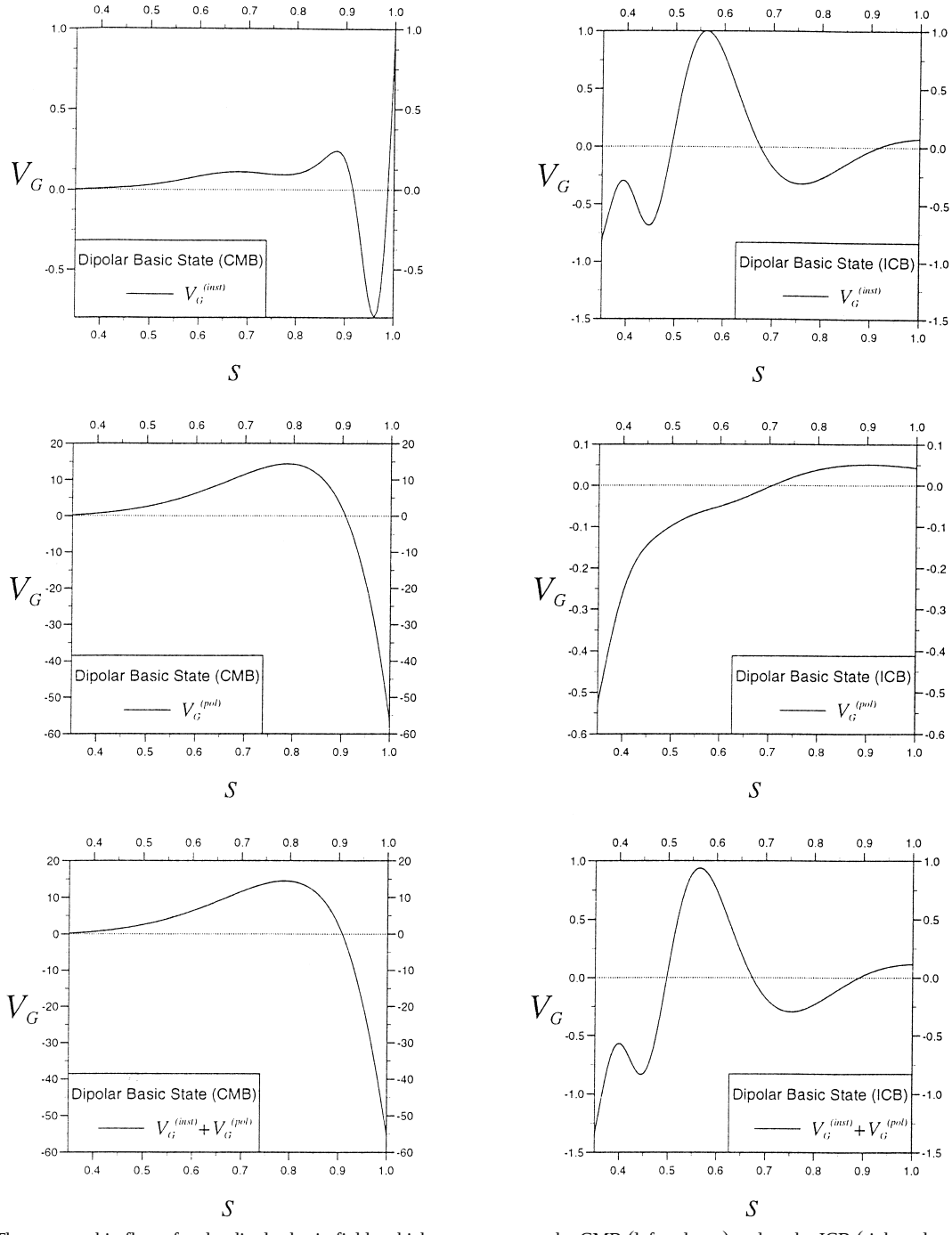

Fig. 4. The geostrophic flows for the dipolar basic fields which concentrate to the CMB (left column) and to the ICB (right column). Here $V_G^{(pol)}$ and $V_G^{(inst)}$ are as defined in (3.8) and (3.9). Both components have been evaluated at $\Lambda = \Lambda_c$ and scaled with max $|V_G^{(inst)}|$.

is appropriate to our model). I is the net viscous torque acting on $s = s_{ib}$, 1 and FLMO have shown that it must vanish. Our results satisfy their finding (within the bounds of numerical precision).

5.2. Dipole field (ICB)

The s-dependencies of our basic states have, at this point, lain unchanged from those first studies (e.g., Fearn, 1983b). The particular form for F was chosen, so that the basic toroidal field would vanish on the inner and outer core boundaries whilst a parameter α allowed variations on this theme (see Fig. 3.1 in M97 or Fig. 1 in MF98 for examples). It was then possible to gain some insight into how results depended on the choice of basic field. However, the function F, tended to concentrate field *away* from the ICB [as in (3.1)]. We now investigate the form (3.2) for F in a field concentrating to the ICB. The structure of the new basic state can be seen in Fig. 1(iii).

What is immediately obvious from the stability results in Table 2 is that those modes that were most unstable when the 'traditional' form for F, (3.1), was used have now been completely damped by ohmic diffusion. For the azimuthal modes having $m \geq 2$, the energetic Elsasser number Λ' now lies in excess of 2.6 (corresponding to $\Lambda \geq 65$) and the most unstable mode is now the $m = 1$ mode.

The difference can be explained in the following way. We know that any instability will tend to concentrate where the basic field is strongest and our new choice of s-dependence has forced the instability towards the ICB. Since the ∇^2 operator scales with s^{-2}, then it will be more effective at damping instabilities which concentrate towards the ICB. Now,

Table 2
Critical parameter values using F in (3.2)

m	1	≥ 2
Λ'_c	1.633	> 2.6
	0.8138	*0.7242*
ω_c	1.318×10^{-3}	–
Modes	ℰ	–
Bifurcation	Sub	–

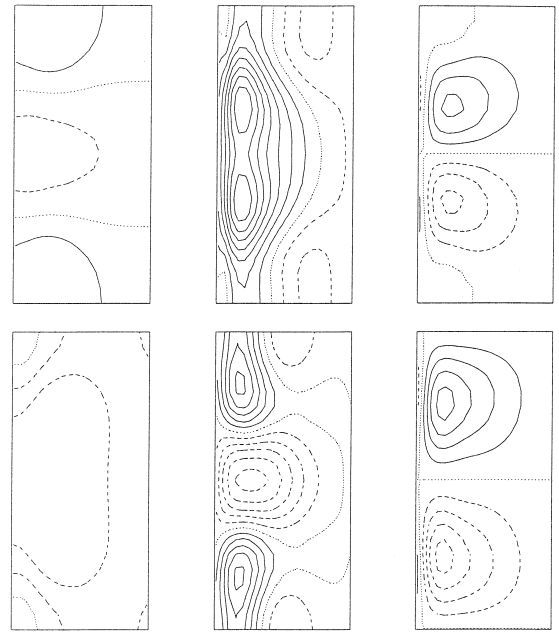

Fig. 5. For basic dipolar field concentration to the ICB: Top row: the real parts of (i) b_s, (ii) b_ϕ and (iii) b_z. The corresponding imaginary parts are shown in the bottom row. All plots share the same contour interval.

ohmic diffusion acts on modes which contain a lot of structure (essentially, the $\nabla^2\mathbf{b}$ becomes large wherever there are strong changes in the gradient of the field, i.e., where the field contains a lot of structure). Therefore, higher order modes concentrating towards the ICB will be damped the most. This explains why the most unstable mode is the $m = 1$ instability and $\Lambda'_c = 1.633$ as opposed to $m = 4$ and $\Lambda'_c = 0.4955$ in the case of field concentration towards the CMB. The effect of field concentration to the ICB is a stabilising one. The eigenfunctions for the field and flow may be seen in Figs. 5 and 6.

Although the most unstable mode retains its quadrupolar symmetry, the simple effect of concentrating field to the ICB has slightly increased Λ'_c, swapped the most unstable mode and drastically reduced the frequency from -11.93 to 3.284×10^{-3} —the instability is now almost stationary. The nonlinear effect of the geostrophic flow still remains subcritical.

It is worth observing that the addition of this section's dipolar modulation to a previously z-inde-

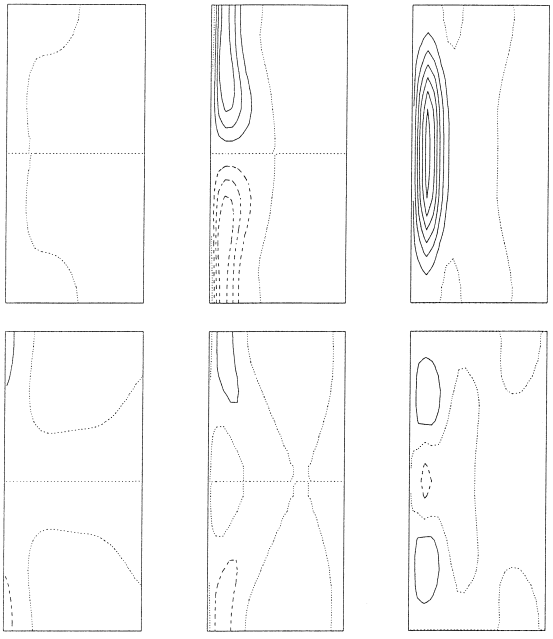

Fig. 6. For basic dipolar field concentration to the ICB: Top row: the real parts of (i) v_s, (ii) v_ϕ and (iii) v_z. The corresponding imaginary parts are shown in the bottom row. All plots share the same contour interval.

pendent basic field [i.e., in MF98, field (3.2)] has stabilised the system. This contrasts the destabilising result of Section 5.1.

6. Conclusions

The work done in this paper analysed the linear and nonlinear stability of a variety of dipolar and quadrupolar basic state fields. The magnetostrophic approximation was employed insofar as viscous boundary layers were retained on the flat bounding plates at $z = \pm\zeta$. The viscous drag from these boundary layers is balanced by the magnetic torque over concentric circular cylinders leading to a determination of the geostrophic flow. We showed in MF98 that the geostrophic flow is the first nonlinear effect to act on an exponentially growing solution to the linear problem. For z-independent basic field configurations, we discovered subcritical instabilities for certain cases of basic fields and aspect ratios. In the viscous analyses of HF1,2 at finite Ekman number, $E = 10^{-4}$, no subcritical instabilities were found.

In this work, we showed that a new constraint on the basic state field and magnetic instability must be satisfied. The axial component of the curl of the linearised Lorentz force must vanish when integrated over the height of the annular container. This is satisfied by any s-dependent basic state and its associated instability, but only by certain s- and z-dependent basic fields and their associated instabilities. For example, a quadrupolar instability must accompany a dipolar azimuthal basic field and a dipolar instability must accompany a quadrupolar basic field to be certain that the consistency condition (4.4) is satisfied. For the other combinations of basic field and instability, any results obtained may or may not be consistent with (4.4) and the restoration of some form of viscosity in the perturbation equations will be needed to resolve this problem.

In this work, we ask the question: do the magnetostrophic results of FLMO and MF98 carry over to more geophysically realistic field configurations, and if so, how do the results compare with the corresponding viscous problem considered by HF3,4? To answer these questions, we used the energetic Elsasser number Λ' defined on a field's total magnetic energy [see (5.1)]. This allowed us to consistently compare the different basic fields of this work and of MF98.

The introduction of an axial dependence on to a z-independent basic field was found to have a destabilising effect for dipolar basic fields concentrating to the CMB and a stabilising effect for the dipole fields concentrating to the ICB and all quadrupolar basic fields. This result is intriguing in that the observed geomagnetic field exhibits a dipolar-type symmetry which can be more susceptible to magnetic instabilities than the quadrupole type. In each case of $\mathscr{D}$- and $\mathscr{E}$-basic fields, given in Section 5, the most unstable mode was the $m = 4$ mode and its nonlinear bifurcation due to V_G was found to be subcritical.

The addition of a magnetic wind (driven by the basic state) was found not to make any significant difference to stability results (with or without the geostrophic flow). Also, a modification of the aspect ratio was very mildly stabilising. Apart from these small differences, the addition of the magnetic wind

and the modification of the aspect ratio did not produce significantly different results to warrant their inclusion here.

For stability analyses in the past, only certain forms of basic field have been considered. Specifically, those that concentrate field to the CMB. We have shown that $\mathscr{D}$- and $\mathscr{E}$-fields concentrating to the ICB changes the most unstable mode. We have shown that the $m = 1$ instability becomes preferred as field concentrates more towards the ICB. This can be understood in terms of the amount of ohmic diffusion experienced by a mode as it approaches the axis of rotation. On comparison with the equivalent basic field concentrating to the CMB, fields concentrating to the ICB showed azimuthal modes becoming heavily damped by ohmic diffusion. What was surprising was that as the higher order modes were becoming stabilised, the $m = 1$ mode was *destabilised* under the $\mathscr{D}$-basic field.

We found that the geostrophic flow was dominated by its mean poloidal field contribution when basic fields concentrating to the CMB were used. The reverse was found to be true for fields concentrating to the ICB (there, V_G was dominated by its contribution from the magnetic instability). This result is interesting in the light of a similar calculation in a spherical geometry carried out by Fearn et al. (1994). They found in a magnetoconvection analysis in a spherical geometry that the contribution from the mean poloidal field was negligible. This would seem to suggest that its contribution could be neglected in general. However, our finding shows that the mean poloidal field's contribution to V_G cannot simply be ignored and is sensitive to the basic state field used.

An important question that we posed was as to whether the qualitative difference between the viscous analysis of HF1,2 and the magnetostrophic analysis of MF98 or FLMO would carry over to more relevant field configurations. The answer is yes. Under the magnetostrophic approximation, the top and bottom no-normal-flow boundary conditions become degenerate. This leaves a two-dimensional 'undetermined' geostrophic flow unlike in the sphere where the boundary conditions are linearly independent. We have chosen to set the non-axisymmetric component of $V_G = 0$ for numerical tractability and for physical realism. However, there is no mathematical reason why this should be so. Further work is needed to resolve the undetermined component. In the viscid calculations of HF1–4, the geostrophic flow is calculated implicitly and will naturally incorporate a non-axisymmetric component if it exists. How important this component was to HF1–4 is difficult to say. However, from Fig. 4 in HF4, it is evident that there is a distinct z-dependence in their U_ϕ and U_s solutions (the axisymmetric flow solutions) just in excess of neutral stability. At their value of the Ekman number, $E = 10^{-4}$, this indicates the equal importance of other nonlinear effects, of whom, we would not expect to see at, lower, more geophysically realistic values of E. Therefore, an explanation for the qualitative difference between HF1–4 and this work is that in our work, V_G is the only nonlinear effect and in HF1–4, the Ekman number E is not sufficiently small for it to be dominant.

Although a cylindrical geometry initially seems more numerically tractable than the spherical geometry, we have found that it leads to hidden complications (in both the linear and nonlinear regimes) that do not arise in the geophysically relevant spherical shell. To this end, care must be exercised when a cylindrical geometry is used, especially when certain aspects of the physics are expected to carry over to the spherical shell geometry.

Acknowledgements

Douglas R. McLean would like to thank the Engineering and Physical Sciences Research Council for funding this investigation through a research studentship, award reference number 95007114. David R. Fearn's work is supported by PPARC grant GR/K 06495.

References

Abramowitz, M., Stegun, I.A., 1965. Handbook of Mathematical Functions. Dover, New York.

Acheson, D.J., 1972. On the hydromagnetic stability of a rotating fluid annulus. J. Fluid Mech. 52, 529–541.

Acheson, D.J., 1973. Hydromagnetic wavelike instabilities in a rapidly rotating stratified fluid. J. Fluid Mech. 61, 609–624.

Acheson, D.J., 1983. Local analysis of thermal and magnetic instabilities in a rapidly rotating fluid. Geophys. Astrophys. Fluid Dyn. 27, 123–136.

Cowling, T.G., 1934. The magnetic field of sunspots. Mon. Not. R. Astr. Soc. 94, 39–48.

Fearn, D.R., 1983a. Boundary conditions for a rapidly rotating hydromagnetic system in a cylindrical container. Geophys. Astrophys. Fluid Dyn. 25, 65–75.

Fearn, D.R., 1983b. Hydromagnetic waves in a differentially rotating annulus: I. A test of local stability analysis. Geophys. Astrophys. Fluid Dyn. 27, 137–162.

Fearn, D.R., 1984. Hydromagnetic waves in a differentially rotating annulus: II. Resistive instabilities. Geophys. Astrophys. Fluid Dyn. 30, 227–239.

Fearn, D.R., 1985. Hydromagnetic waves in a differentially rotating annulus: III. The affect of an axial field. Geophys. Astrophys. Fluid Dyn. 33, 185–197.

Fearn, D.R., 1988. Hydromagnetic waves in a differentially rotating annulus: IV. Insulating boundaries. Geophys. Astrophys. Fluid Dyn. 44, 55–75.

Fearn, D.R., 1994. Nonlinear planetary dynamos. In: Proctor, M.R.E., Gilbert, A.D. (Eds.), Lectures on Solar and Planetary Dynamos. Cambridge Univ. Press, pp. 219–244.

Fearn, D.R., 1997. The geodynamo. In: Crossley, D. (Ed.), Earth's Deep Interior. Gordon and Breach, London, pp. 79–114.

Fearn, D.R., Proctor, M.R.E., Sellar, C.C., 1994. Nonlinear magnetoconvection in a rapidly rotating sphere and Taylors' constraint. Geophys. Astrophys. Fluid Dyn. 77, 111–132.

Fearn, D.R., Lamb, C.J., McLean, D.R., Ogden, R.R., 1997. The influence of differential rotation on magnetic instability and nonlinear magnetic instability in the magnetostrophic limit. Geophys. Astrophys. Fluid Dyn. 86, 173–200.

Glatzmaier, G.A., Roberts, P.H., 1995a. A three-dimensional convective dynamo solution with rotating and finitely conducting inner core and mantle. Phys. Earth Planet. Inter. 91, 63–75.

Glatzmaier, G.A., Roberts, P.H., 1995b. A three-dimensional self-consistent computer simulation of a geomagnetic field reversal. Nature 377, 203–209.

Glatzmaier, G.A., Roberts, P.H., 1996. Rotation and magnetism of the Earth's inner core. Science 274, 1887–1891.

Glatzmaier, G.A., Roberts, P.H., 1997. Simulating the geodynamo. Contemp. Phys. 38, 269–288.

Gubbins, D., Zhang, K., 1993. Symmetry properties of the dynamo equations for palaeomagnetism and geomagnetism. Phys. Earth Planet. Inter. 75, 225–241.

Hollerbach, R., 1996. On the theory of the geodynamo. Phys. Earth Planet. Inter. 98, 163–185.

Hutcheson, K.A., Fearn, D.R., 1995a. The nonlinear evolution of magnetic instabilities in a rapidly rotating annulus. J. Fluid Mech. 291, 343–368.

Hutcheson, K.A., Fearn, D.R., 1995b. Nonlinear stability of the geomagnetic field. Geophys. Res. Lett. 22, 1637–1640.

Hutcheson, K.A., Fearn, D.R., 1996. The stability of toroidal magnetic fields with equatorial symmetry: implications for the Earth's magnetic field. Phys. Earth Planet. Inter. 97, 43–54.

Hutcheson, K.A., Fearn, D.R., 1997. The stability of toroidal magnetic fields with equatorial symmetry: evolution of instabilities. Phys. Earth Planet. Inter. 99, 19–32.

Jault, D., 1995. Model Z by computation and Taylor's condition. Geophys. Astrophys. Fluid Dyn. 79, 99–124.

Kuang, W., Bloxham, J., 1997a. An Earth-like numerical dynamo model. Nature 389, 371–374.

Kuang, W., Bloxham, J., 1997b. Numerical modelling of magnetohydrodynamic convection in a rapidly rotating spherical shell: weak and strong field dynamo action. J. Comp. Phys., submitted.

Malkus, W.V.R., Proctor, M.R.E., 1975. The macrodynamics of α-effect dynamos in rotating fluids. J. Fluid Mech. 67, 417–443.

McLean, D.R., 1997. Magnetohydrodynamic instabilities in a rapidly rotating system. PhD Thesis, Department of Mathematics, University of Glasgow.

McLean, D.R., Fearn, D.R., 1999. The geostrophic nonlinearity and its effect on magnetic instability. Geophys. Astrophys. Fluid Dyn., In Press.

Taylor, J.B., 1963. The magnetohydrodynamics of a rotating fluid and the Earth's dynamo problem. Proc. R. Soc. London A 274, 274–283.

Zhang, K., 1995b. Spherical-shell rotating convection in the presence of a toroidal magnetic field. Proc. R. Soc. London A 448, 245–268.

Zhang, K., Fearn, D.R., 1994. Hydromagnetic waves in rapidly rotating spherical shells generated by magnetic toroidal decay modes. Geophys. Astrophys. Fluid Dyn. 77, 133–157.

Zhang, K., Fearn, D.R., 1995. Hydromagnetic waves in rapidly rotating spherical shells generated by magnetic poloidal decay modes. Geophys. Astrophys. Fluid Dyn. 81, 193–209.